Geophysical Research Letters
MOIS ANNEE; 31(13) : NIL_27-NIL_30
http://dx.doi.org/10.1029/2004GL019848

An edited version of this paper was published by AGU.

Large gas hydrate accumulations on the eastern Nankai Trough inferred from new high-resolution 2-D seismic data

H. Nouzé[1], P. Henry[2], M. Noble[3], V. Martin[2], and G. Pascal[2]

1 Ifremer Centre de Brest, Géosciences Marines, BP70, 29280 Plouzané Cedex, FRANCE.
2 Laboratoire de Géologie UMR 8538, Ecole Normale Supérieure, Paris, FRANCE.
3 Ecole des Mines de Paris, Centre de Recherche en Géophysique, 35 rue St Honoré, 77305 Fontainebleau Cedex, FRANCE.

*: Corresponding author : H. Nouzé, Ifremer DROGM, BP 70, 29280 Plouzané, France
Tel.: (33) (0)2 98 22 47 09 – Fax.: (33) (0)2 98 22 45 49 – e-mail: hnouze@ifremer.fr

Abstract:

Previous studies have revealed the presence of a widespread Bottom Simulating Reflector (BSR) on the eastern Nankai slope, as well as the occurrence of enigmatic high amplitude reflections that extend well above the BSR. New high-resolution 2-D seismic data were collected on the eastern Nankai slope, during the French-Japanese SFJ cruise in year 2000 and AVA analyses of the enigmatic reflectors are conducted. At the studied location, these analyses suggest that high amplitude anomalies above the BSR delineate the top of gas hydrate rich sediments. Several tens % of the sediment porosity would be filled with gas hydrates between the BSR and a sharp boundary 30 to 60 m above. To account for these observations, we propose that an invasion by free gas of the present day gas hydrate stability zone occurred in the past. Several mechanisms for this intrusion are discussed.

Introduction

The occurrence of marine gas hydrates in the sediments is mainly inferred from the observation on seismic sections of a Bottom Simulating Reflector (BSR). Geophysical studies (e.g. Hyndman et al., 1992) have shown that the BSR are generated at the transition between sediments containing a variable amount of solid gas hydrate above, and sediments containing a small volumetric fraction, of free gas below. The BSR is thus generally interpreted (Hyndman et al., 1992) as the Base of the Gas Hydrate Stability zone (BGHS). The stability field for gas hydrate being mainly P-T dependant, and isotherms approximately parallel to the sea floor, the BSR parallels the seabed and often cuts across sedimentary layer reflections. The P and S wave velocities of pure gas hydrate (Sloan, 1998) are high in comparison with the average P and S wave velocities in shallow marine sediments. Thus, the transition between normal and gas hydrate bearing sediments should theoretically generate a seismic reflection above the BSR, providing that the thickness of this transition is less than a wavelength of the seismic signal. However there is no account of the observation of such a reflection in the literature. This leads authors to propose that this transition must be, at the studied sites, gradational (e.g. Fink and Spence, 1999). In this paper, we focus our attention to some particular reflections (referred to as Anomalous Amplitude Reflections and noted AAs in the following) observed on new high resolution seismic data on the upper slope of the eastern Nankai margin. Based on data interpretation and on amplitude versus angle analyses (AVA) of these reflections, we propose that they represent a sharp interface between normal sediments and the top of sediments with high hydrate content.

BSR on the eastern Nankai slope

The Nankai Trough extends about 700 km from the Suruga Trough to the northern end of the Kyushu-Palau ridge. The Philipine Sea plate is subducting northwestward beneath the Eurasian plate at about 2-4cm/yr along the trough (Seno et al., 1993). In this area, the position of the BGHS could have been influenced by 1/ tectonic uplift and subsidence and 2/ sea level and water temperature changes. Tectonic events controlled by the subduction of basement ridges occur on a time scale of 100 000 years to 1 M years (Mazzotti et al., 2002) with uplift rates of several mm/year. Sea water temperature variations occur on a shorter time scale, notably in relation with the variability of the Kuroshio current (Sawada & Handa, 1998).

BSRs are commonly observed on the eastern Nankai margin (Ashi et al., 2002; Foucher et al., 2002), in water depths ranging from 3 km to about 700 m (fig. 1), from the outer portion of the accretionary prism to the flanks of the Kodaiba and Daichii-Tenryu knolls on the upper slope. On the southern flank of the Daichii-Tenryu Knoll, Foucher et al. (2002) report the occurrence of what they refer to as a double BSR. They interpret the upper BSR as an active methane hydrate BSR and suggest that the lower BSR is a residual BSR. This could have followed a recent migration of the base of the methane hydrate stability zone, in response to recent sea bottom warming or tectonic uplift.

Data source

JNOC Nankai well

An exploratory well was drilled on the Nankai slope (fig. 1) at 945m water depth (Takahashi et al., 2001). The top 100 m unit is flat lying mudstone-siltstone with occurrences of ash beds. The lower unit is gently dipping mudstone with increasing number of sandstone beds above the BSR. Gas hydrates, usually < 1mm in diameter, occurs predominantly as pore filling of sandy and silty layers around 200-to 270 mbsf, but mudstone is substantially hydrate free. An estimate of the gas hydrate saturation was obtained from the resistivity log. The major gas hydrate zones correspond to sandy layers, with up to 70-80% hydrate saturation, whereas in mudstone layers the gas hydrate saturation is less than 10%. The porosity (Matsumoto, 2002) is almost constant with a value of about 45% from the sea bottom down to the BSR level, except for the sandy layers where a porosity reduction to 36% is observed. Gas analyses (Matsumoto, 2002) at the BSR level in the JNOC hole reveal that gases are mainly microbial methane. However in situ methane generation in the host Pleistocene sediments (TOC~0.5%) is not enough to accumulate the observed amount of hydrate” (Ashi et al., 2002).

Seismic data

This study is based on the analysis of high resolution seismic data recorded on a 4.5 km long streamer towed at 15 m immersion during the SFJ cruise on N/O Nadir in year 2000. The source was composed of an array of G-I and mini G-I guns, with a total volume of 151 $inch^3$ at 1.5 m depth. The processing sequence that has been applied to the data (fig. 2 and 3) includes source delay correction (37ms), band-pass filtering (20-300 Hz), and spherical divergence correction. A preserved amplitude pre-stack depth migration algorithm was used, especially to handle 2-D velocity structures and obtain depth sections of our survey area.

Although the new data enable better imaging (fig. 2 and 3), they do not bring significant new information about the BSR and double BSR features. Conversely, they enable better characterisation of the AAs above the BSR. The analyses were conducted on line SFJHR01 where the AAs were the most clearly detectable (fig. 3a). They root at the BSR level and can be traced at between 30 to 60 m above the BSR. Close to CDP 1570, they appear as a distinct high amplitude reflector with a polarity corresponding to the seafloor polarity (fig. 3b) that cross cuts the stratigraphy, whereas between km 7 and km 10, they show off as short segments of stratigraphic reflectors with normal polarity and enhanced amplitude. These observations rule out the hypothesis that the AAs could be caused by a sedimentary discontinuity. On CDP gathers (fig. 3b) they have low amplitude at near offsets and exhibit a sudden change in amplitude at about 1 km offset.

AVA analyses

AVA analyses determine the changes in P-wave reflection amplitude as a function of reflection angle. These changes depend on the shear (Vs) and compressional (Vp) wave velocities as well as densities above and below the reflecting interface.

To estimate the reflection coefficients for the studied reflectors the approach described in Nouzé & Baltzer. (2003) was used: 1/ the amplitude of both the sea bottom and the reflectors is picked on the pre-stack CDP data, 2/ the sea floor amplitudes are corrected for spherical divergence attenuation, 3/ the zero offset sea floor reflection coefficient and the density at the sea floor are used to obtain Vp at the seafloor and to model the AVO sea floor response 4/ angular dependant source and receiver amplitude corrections are derived by dividing the theoretical sea floor response by the actual sea floor amplitudes, 5/ for a given reflector and for each offset, a ray tracing algorithm is run to obtain the values of the incidence angles for the reflections at the studied reflector, the transmission losses at the interfaces of the model, as well as the attenuation due to energy absorption in the sediments, 6/ the amplitudes of the studied reflectors are corrected for spherical divergence, source and receiver effects, attenuation and transmission losses.

The sea floor zero offset reflection coefficient (#0.27) was calculated by dividing the divergence corrected amplitude of the sea floor by the one of the sea floor first multiple. No measurements being available, the P wave attenuation Qp was set to a value of 100 at the seafloor and 200 at the BSR level, which is consistent with values obtained in other studies (Ayres & Theilen, 2001). Vs for the sediments (fig. 4) without gas or gas hydrates were estimated according to the formulas given by Hamilton (1976) for water saturated silt clays and turbidites. Vp for the sediments without gas or gas hydrates (fig.4) at the AAs level were derived from the stacking velocities, assuming that the sediments are free of gas or gas hydrate. The porosity was extracted from the JNOC hole porosity log (Matsumoto, 2002). Unless grain contact cementation by hydrate is hypothesized to occur at a low hydrate concentration (less than 10%), most recently developed models, either empirical or based on physical theories yield comparable variations of Vp and Vs with hydrate concentration (Guerin et al., 1999). The Tinivella (1999) approach was used to compute Vp and Vs for partially hydrate bearing or gas saturated sediments. It formulates the propagation of seismic waves in terms of wave scattering through a 2 or 3 phase medium. In particular, this model does no require an *a priori* assumption about grain contact cementation. Please refer to Tinivella (1999) for a detailed description of the model. The AVO responses have been computed using the full Zoeppritz equations (Zoeppritz, 1919).

Results

AVA analysis of the AAs has been conducted on CDPs 1560, 1570, and 1580. The results are presented on figure 5. For angles between 40° and 50°, the reflection coefficient of the AAs increases dramatically from a value of about 0.1 to about 0.9. To account for such a strong increase, important sediment properties variations are needed. Two hypotheses have been tested: 1/ normal sediments above hydrate bearing sediments 2/ sediments containing free gas above normal sediments. The main effect of free gas in the sediments, either with a uniform or patchy distribution, is to decrease the P-wave velocity. In order to explain the strong increase of the coefficients between 40 and 50° of incidence angle, relatively high gas content is needed (fig. 5), but then, the reflection coefficient at normal incidence will be increased and will not fit the observed data. On the contrary, the modelled AVA behaviour of the reflection at the transition between normal and gas hydrate bearing sediments (between 40% and 60% gas hydrates in the porosity) fits the data very well, including the strong increase for incidence angles between 40° and 50°.

Discussion and conclusion

The AVA analyses are based on the assumption of a sharp boundary between two homogenous media and an assumed attenuation. However, the analyses are sufficient to rule out the hypothesis that the AAs are caused by free gas and suggest that the anomalies are most likely caused by large gas hydrate accumulations (several tens %) in the first 30 to 60 m metres above the BSR. Such accumulations were also inferred from resistivity and chlorinity measurements at the nearby JNOC hole (Matsumoto, 2002), however no AAs are observed on the seismic data at this site.

Observation of a relatively narrow gas hydrate rich layer immediately above the BSR is hard to reconcile with hydrate formation models from methane in solution and would be better explained by free gas migration into the BGHS. In principle, the observation of a sharp transition at the top of hydrate rich sediments could result from steady-state advection-diffusion models (Xu & Ruppel, 2000). However, these models would generally predict a broader zone of hydrate occurrence, or lower hydrate concentrations (Davie & Buffet, 2001), this regardless of whether the methane is produced in situ, advected from depth or recycled at the BGHS.

Several studies suggest that free gas may exist within the hydrate stability zone if the hydrate shields the gas form the pore water or if pore water salinity is increased by hydrate formation. These processes have been proposed to explain localised gas flow through the hydrate stability zone (Clennell et al., 1999; Gorman et al., 2002).

We suggest that the same processes may occur in a more distributed way within coarse grained sedimentary layers. Gas could then only migrate where hydrate concentration exceeds a certain threshold and a sharp front is thus obtained at the top of the gas invaded zone. This model could explain the high hydrate concentrations and the sharp reflective top of the hydrate bearing sediments. If the gas migration is a transient process, no free gas remains once all the gas has been converted to hydrate.

Alternatively, the BGHS may have been located at a higher level in a recent past. In this hypothesis, the accumulation would form as gas trapped below the downward migrating BSR is converted to hydrate. It is unclear how a local downward migration could be obtained but we cannot rule out a local thermal anomaly related to transient fluid (water and/or gas) flow.

Acknowledgements

The SFJ cruise was conducted in the framework of the french-japanese program Seize. We are grateful to Captain Remy Balcon, the officers and crew from the N/O Le Nadir for their cooperation during the SFJ cruise. The authors would like to thank as well the sponsors of the DIG consortium of the Ecole des Mines de Paris for their support.

References

Ashi, J., Tokuyama, H., and Taira, A., Distribution of methane hydrate BSRs and its implication for the prism growth in the Nankai Trough, Marine Geology, 187, 177-191, 2002.

Ayres, A., Theilen, F., Preliminary laboratory investigations into the attenuation of compressional and shear waves on near-surface marine sediments, Geophysical Prospecting, 49(1), 120-127, 2001.

Clennell, M.B., Hovland, M., Booth, J.S., Henry, P., Winters, W.J., Formation of natural gas hydrates in marine sediments; 1, Conceptual model of gas hydrate growth conditioned by host sediment properties, J. Geophys. Res., 104, 22,985-23,003, 1999.

Davie, M. K., & Buffet, B. A., A numerical model for the formation of gas hydrates below the seafloor, JGR 106, pp. 497-514, 2001.

Fink, C.R., & Spence, GD., Hydrate distribution off Vancouver Island from multi-frequency single channel seismic reflection data, J. Geophys. Res., 104, 2909-2922, 1999.

Foucher, J.P., Nouzé, H., Henry, P., Observation and tentative interpretation of a double BSR on the Nankai slope, Marine Geology, 187, 161-175, 2002.

Gorman, A.R., Holbrook, W.S., Hornbach, M.J., Hachwith, K.L., Lizarralde, D., Pecher, I., Migration of methane gas through the hydrate stability zone in a low flux hydrate province, Geology, 30, 327-330, 2002.

G., Guerin, D., Goldberg, and A., Meltser, Characterisation of in situ elastic properties of gas hydrate bearing sediments on the Blake Ridge, J. Geophys. Res., 104, 17,781-17,795, 1999.

Hamilton, E. L., Shear-wave velocity versus depth in marine sediments: a review, Geophysics, 41, 985-996, 1976.

Hyndman, R.D., Foucher, J.P., Yamano, M., Fisher, A. and Scientific Team of Ocean Drilling Program Leg 131, Deep sea bottom-simulating reflectors: calibration of the base of the hydrate stability field as used for heat flow estimates, Earth Planet. Sci. Lett., 109: 289-301, 1992.

Matsumoto, R., Comparison of Marine and Permafrost Gas Hydrate: Examples from Nankai Trough and Mackensie Delta, in: 4^{th} int. conf. on gas hydrate proc., Yokohama, Japan, 2002.

Mazzotti, S., Lallemant, S.J., Henry, P., Le Pichon, X., Tokuyama, H., Takahashi, N., Intraplate shortening and underthrusting of a large basement ridge in the eastern Nankai subduction zone, Marine Geology, 187, 63-88, 2002.

Nouzé, H. & Baltzer, A., Shallow bottom-simulating reflectors on the Angola margin, in relation with gas and gas hydrate in the sediments. Van Rensbergen, P. Hillis, R. Maltman , A. Morley (eds), Subsurface sediment mobilization, Geological Society, London, special publications, 216, 191-206, 2003.

Sawada, K. & Handa, N., Variability of the path of the Kuroshio ocean current over the past 25000 years, Nature, 392: 592-594, 1998.

Seno, T., Stein, S., Gripp, A.E., A model fort he motion of the Philippine Sea plate consistent with NUVEL-1 and geological data, J. Geophys. Res. 98, 17941-17948, 1993.

Sloan, E.D.J., Clathrate hydrates of natural gases, second edition, revised and expansed, Chemical Industries, 73. Marcel Dekker, Inc., New York, 705 pp., 1998.

Takahashi, H., Yonezawa, T., and Takedomi, Y., Exploration for natural hydrate in Nankai trough wells offshore Japan, in Offshore Technology Conference 2001, Houston, USA, ref. OTC 13040, 2001.

Tinivella, U., A method or estimating gas hydrate and free gas concentrations in marine sediments, Boll. Geofis. Teor. Applic., 40, 19-30, 1999.

Xu, W., & Ruppel, C., Predicting the occurrence, distribution and evolution of methane gas hydrates in porous marine sediment, J. Geophys. Res., 104, 5081-5096, 1999.

Zoeppritz, K., Erdbebenwellen VIII B, On the reflection and penetration of seismic waves through unstable layers: Goettinger Nachr., 66-84, 1919.

Figure captions

Figure 1: Location map of the studied area.

Bathymetric contours every 100m. Thin lines represent the SFJ HR 2D lines. Thick line is line SFJHR01 presented on figure 2.

Figure 2: Depth migrated seismic line SFJHR01.

Figure 3:

Left: 3a) a detail of depth migrated line SFJHR01. Note that the amplitude anomalies do not follow the sedimentary layers (BSR like behaviour)

Right: 3b) wiggle plot of the seafloor and AAs response at CDP 1570 between 700 and 1200m offset. Signature deconvolution has been applied to the data in order to remove the strong ghost effect due to the streamer immersion and horizons have been flattened for display purposes. Note the strong increase of the amplitudes of the AA reflector at about 1000m offset.

Figure 4: Densities, P wave and S wave velocities for the sediments without gas or gas hydrates used in the models.

Figure 5: AAs reflection coefficient versus angle.

Markers: dots=data from CDP 1460; diamonds=data from CDP 1470; stars=data from CDP 1480. Thick lines: normal sediments over hydrated sediments. Thin lines: gassy sediments over normal sediments. See table 1 for the values of the parameters used in the models.

Table

	Norm. Sed.	40% GH	50% GH	60% GH	1% gas	5% gas	10% gas	20% gas
Vp (m/s)	1644	2024	2194	2413	1598	1450	1322	1161
Vs (m/s)	355	615	795	1020	355	357	359	364
density	1,84	1,64	1,59	1,53	1,84	1,82	1,79	1,75

Table 1: Vp, Vs and densities at the AAs depth, used to compute the AVA response of the different models tested. For sediments with gas, a patchy gas distribution has been assumed. Vp and Vs for a 1% uniform gas distribution are roughly equivalent to Vp and Vs for a 10% gas in a patchy distribution.

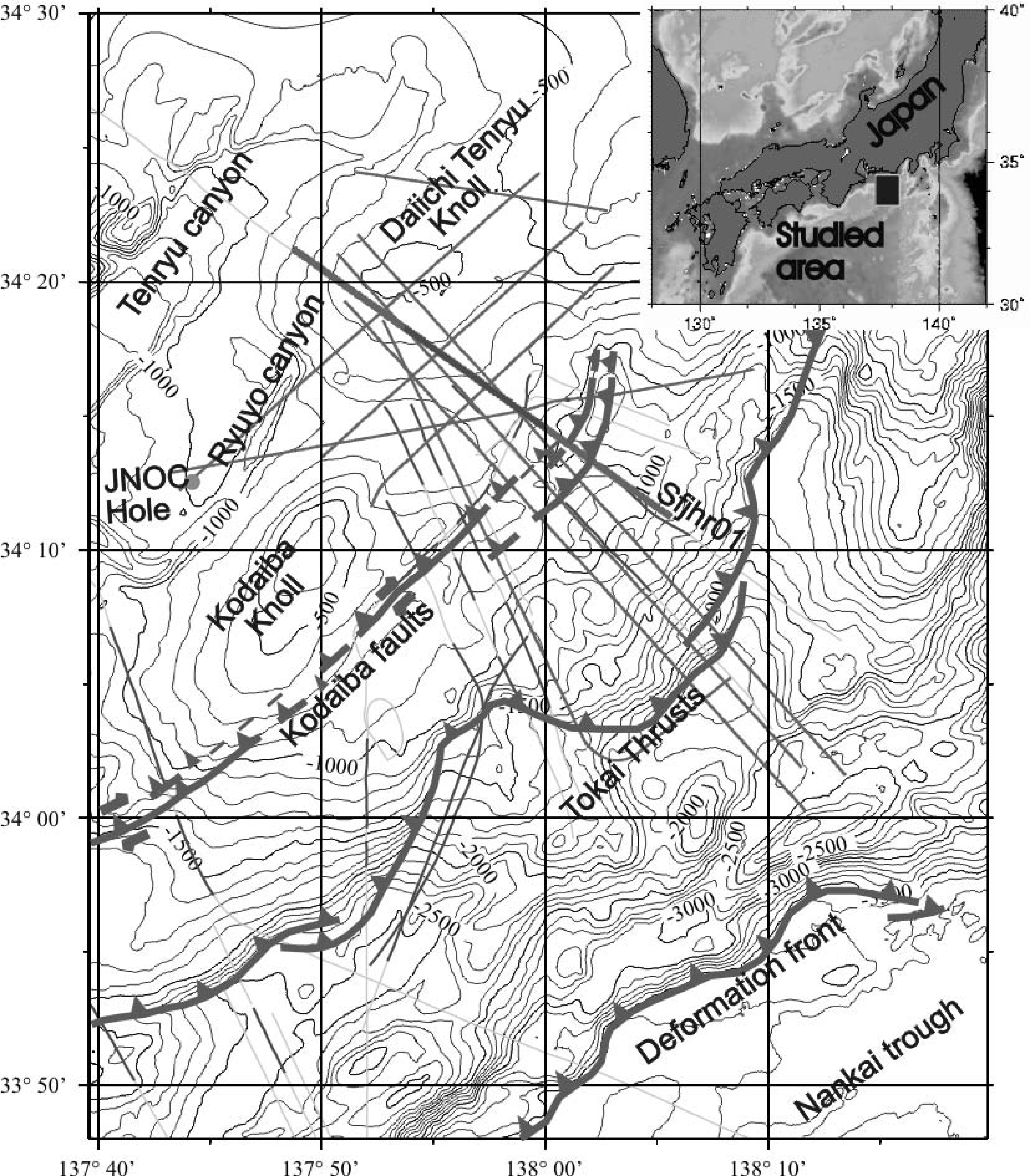

34° 30'
34° 20'
34° 10'
34° 00'
33° 50'
137° 40'
137° 50'
138° 00'
138° 10'
Tenryu canyon
Daiichi Tenryu Knoll
Ryuyo canyon
JNOC Hole
Kodaiba Knoll
Kodaiba faults
Sfjhr01
Tokai Thrusts
Deformation front
Nankai trough
Japan
Studied area
130°
135°
140°
30°
35°
40°
-500
-1000
-1500
-2000
-2500
-3000

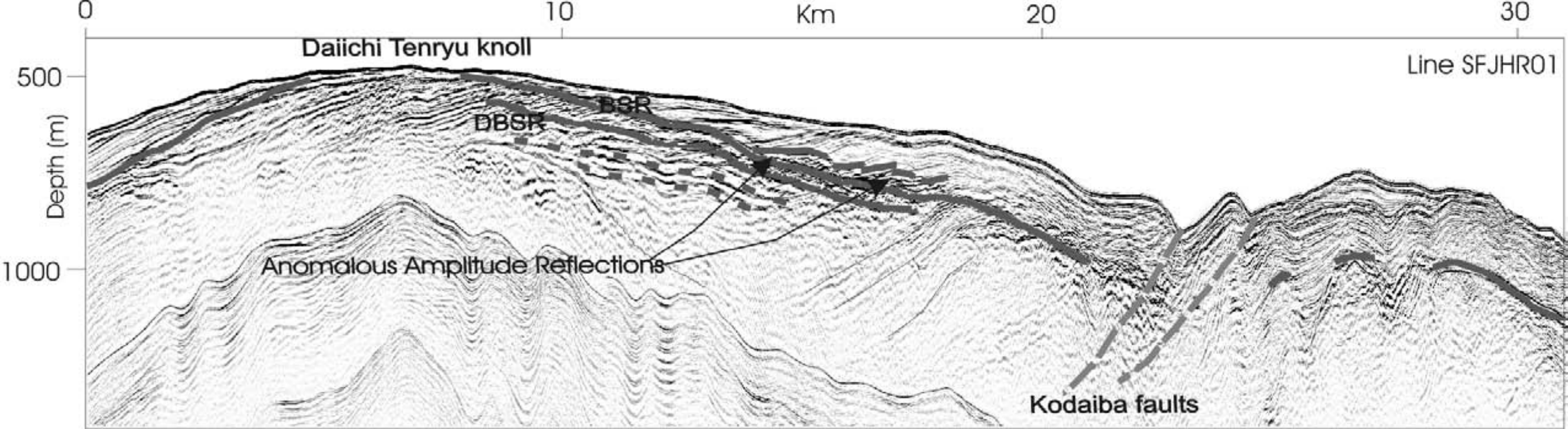

0
10
Km
20
30
Daiichi Tenryu knoll
Line SFJHR01
500
1000
Depth (m)
BSR
DBSR
Anomalous Amplitude Reflections
Kodaiba faults

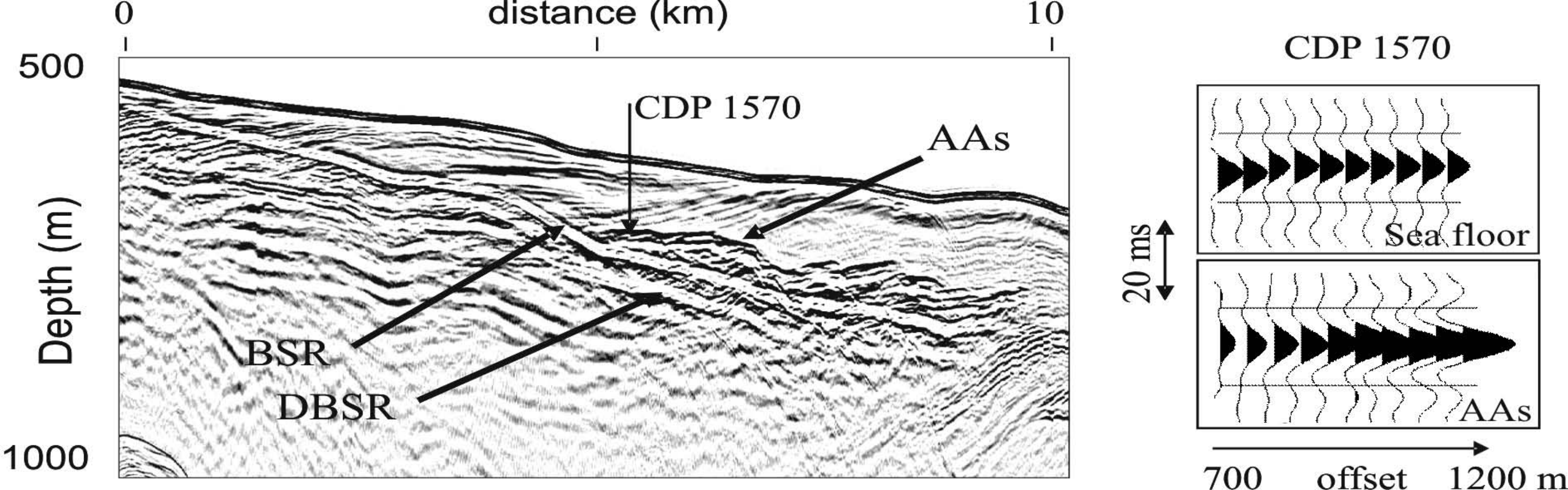

0
distance (km)
10
500
Depth (m)
1000
CDP 1570
AAs
BSR
DBSR
CDP 1570
Sea floor
20 ms
AAs
700
offset
1200 m

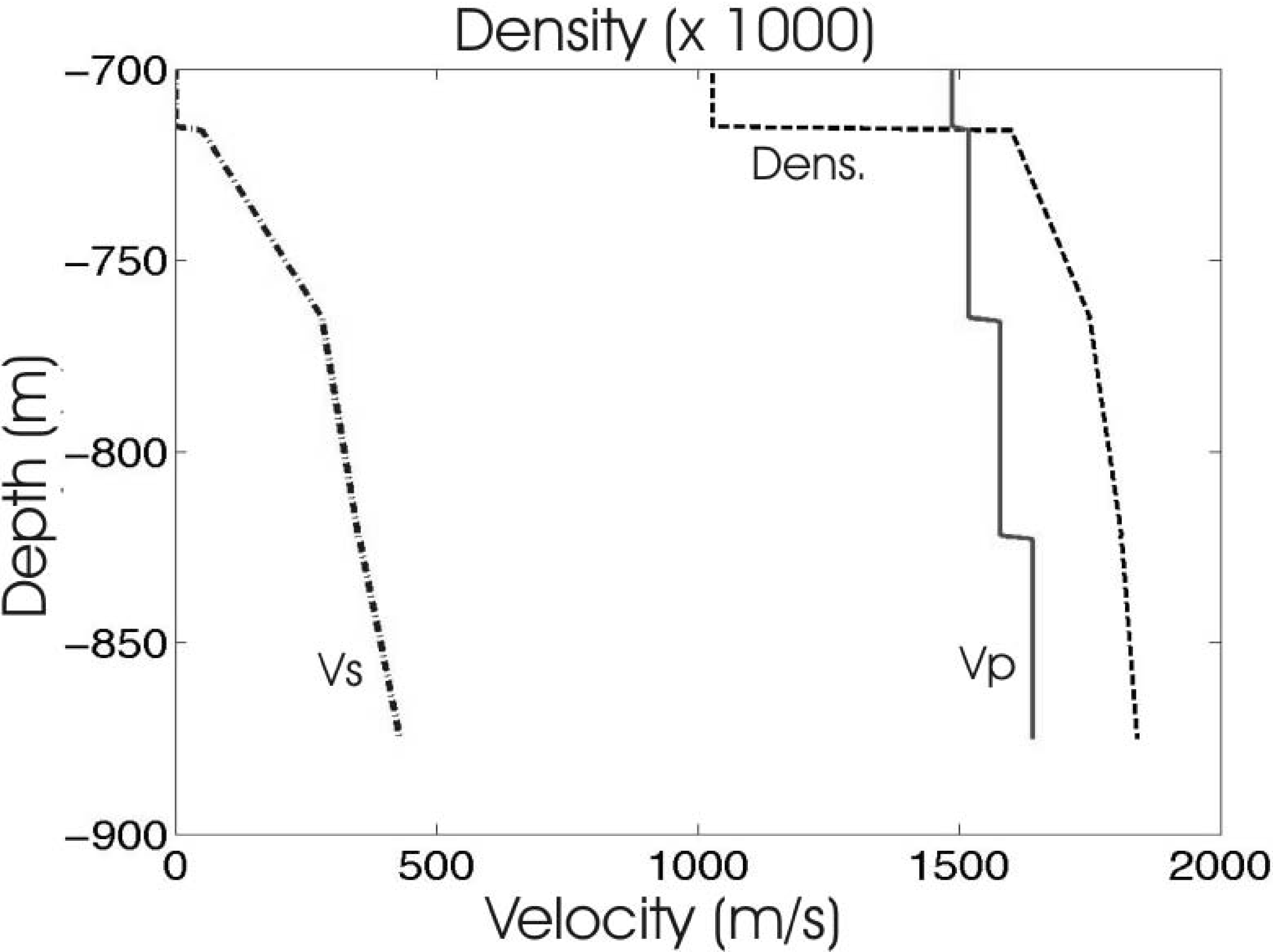
Density (x 1000)
Dens.
Vs
Vp
Depth (m)
Velocity (m/s)
−700
−750
−800
−850
−900
0
500
1000
1500
2000

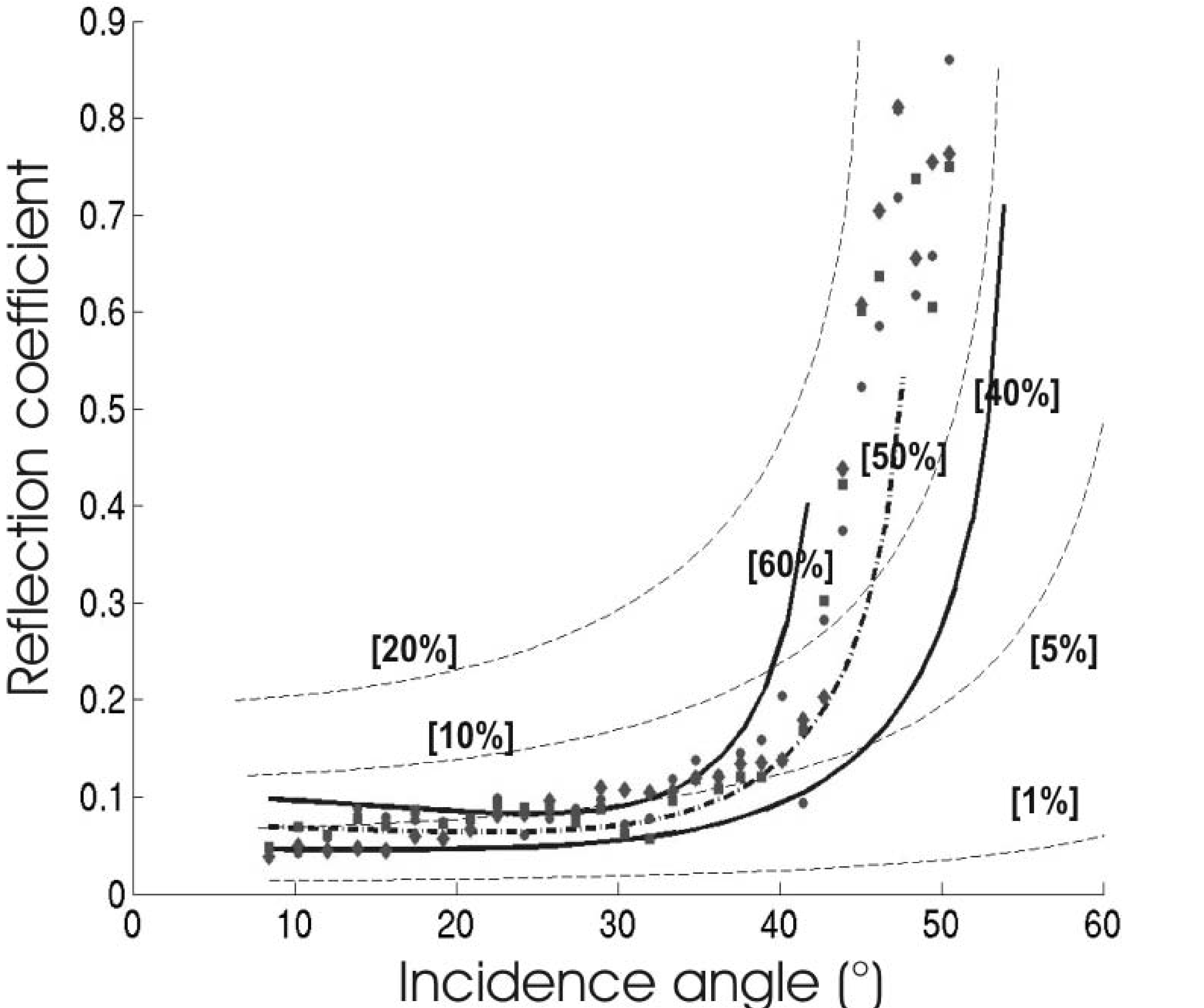

Reflection coefficient
Incidence angle (°)
0.9
0.8
0.7
0.6
0.5
0.4
0.3
0.2
0.1
0
0
10
20
30
40
50
60
[20%]
[10%]
[60%]
[50%]
[40%]
[5%]
[1%]